very close to the basin boundary. If the jump is to the lower blue branch, its magnitude will be approximately $2\sqrt{\varepsilon}$, a macroscopic quantity even at small μ. However, the jump to the upper red branch will change the value of y less than if $\varepsilon = 0$. If the initial $y = -\sqrt{\varepsilon}$, the situation is similar.

- **Case $\varepsilon > \lambda$.** In this case, the system has two sinks at any positive μ. The bifurcation diagram in Fig. 5 at the top right shows that we cannot expect a larger response in y to a jump in μ than in the case $\varepsilon = 0$.

In summary, the most interesting case from the viewpoint of sensor design is $0 < \varepsilon < \lambda$, $\mu > \mu_1^*(\varepsilon)$, as a macroscopic jump in y is possible. But how can one guarantee it will happen? We envision an upgrade of the system shown in Fig. 7.

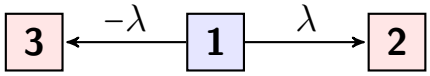

$$\begin{aligned} \dot{x} &= \mu x - x^3, \\ \dot{y} &= (\mu + \varepsilon) y - y^3 - \lambda x, \\ \dot{z} &= (\mu + \varepsilon) z - z^3 + \lambda x. \end{aligned} \tag{10}$$

Figure 7: A schematic of a three-cell network of inhomogeneous pitchfork cells. The proposed coupling can yield a dramatic amplification effect under certain settings.

In the modified system, cell one is coupled to two identical cells, two and three, with coupling coefficients of equal magnitudes but opposite signs. In this case, if μ jumps from zero to a positive value, the response in one of these cells will be significant. To ensure that $\mu > \mu_1^*(\varepsilon)$, we can prescribe the sensitivity threshold μ_0, and choose ε such that $\mu_1^*(\varepsilon) < \mu_0$, i.e.,

$$\varepsilon < \frac{3\mu_0^{1/3}\lambda^{2/3}}{4^{1/3}}. \tag{11}$$

3.4 Singularity theory approach

In this section, we describe changes that occur in the number of equilibrium points and their stability properties from the standpoint of the *singularity theory* [36, 37].

Let $\mu > 0$. We start by assuming that the first cell in Eq. (5) has already converged to a nonzero equilibrium, $x = \pm\sqrt{\mu}$. Since x always converges to an equilibrium point, the dependence of y on x vanishes as x becomes indistinguishable from a constant. Theorem 17.0.3 in [38] makes this precise. We consider the case $x = \sqrt{\mu}$. The case $x = -\sqrt{\mu}$ is treated similarly. The governing ODE for the second cell then becomes

$$\dot{y} = -y^3 + (\mu + \varepsilon) y - \lambda\sqrt{\mu} \equiv p_+(y). \tag{12}$$

The perturbation ε lets the free term and the coefficient of y in the right-hand side of Eq. (12) change independently at any fixed λ. We denote $\lambda\sqrt{\mu}$ by $\hat{\lambda}$ and $\mu + \varepsilon$ by $\hat{\mu}$ and rewrite Eq. (12) as

$$\dot{y} = -y^3 + \hat{\mu} y - \hat{\lambda} =: G(y, \hat{\lambda}, \hat{\mu}) \equiv g(y, \hat{\lambda}) + \hat{\mu} y, \tag{13}$$

where $\hat{\lambda} \in \mathbb{R}$. We treat the function $g(y, \hat{\lambda}) = -y^3 - \hat{\lambda}$ as the main function, or a *germ*, and the term $\hat{\mu} y$ as a perturbation to it. Looking for the equilibria of the unperturbed system $\dot{y} = g(y, \hat{\lambda})$, we solve $g(y, \hat{\lambda}) = 0$ for y and plot y as a function of $\hat{\lambda}$. This germ has a unique root $y = -\hat{\lambda}^{1/3}$. The graph of y versus $\hat{\lambda}$ has a vertical tangent and an inflection point at $\hat{\lambda} = 0$. At this point, $g = g_y = g_{yy} = 0$, which means that this is a *hysteresis point*. The bifurcation diagram at a hysteresis point is not persistent: a small perturbation of the germ changes its root structure.

Singularity theory [36] is a tool for identifying qualitative changes in bifurcation diagrams of germs, i.e., in their root structure, arising from small perturbations. The germ $g(y, \hat{\lambda}) =$

$-y^3 - \hat{\lambda}$ matches the first example in ([36], Section III.4(b)), where it is proven that the function $G(x, \hat{\lambda}, \hat{\mu}) = g(y, \hat{\lambda}) + \hat{\mu} y$ is a *universal unfolding* of g. This means that

1. $G(x, \hat{\lambda}, 0) = g(x, \hat{\lambda})$,
2. $G(x, \hat{\lambda}, \boldsymbol{\alpha})$, $\boldsymbol{\alpha} \in \mathbb{R}^k$, captures all possible qualitative behaviors of the solution branches of $g(x, \hat{\lambda}) + \alpha p(x, \hat{\lambda}, \alpha) = 0$, as $\hat{\lambda}$ runs through the real line, resulting from arbitrary small perturbations one-parameter perturbations $\alpha p(x, \hat{\lambda}, \alpha)$, and
3. k is the minimal number of parameters, in addition to $\hat{\lambda}$, to do so.

In our case, this minimal number of parameters is one. Thus, we find all possible bifurcations of $\dot{y} = G(y, \hat{\lambda}, \hat{\mu})$. The necessary condition for $(y_0, \hat{\lambda}_0, \hat{\mu}_0)$ to be a *singularity*, or a bifurcation point, i.e., a point where the number of the solutions y to $G(y, \hat{\lambda}, \hat{\mu}) = 0$ may change, is

$$G(y_0, \hat{\lambda}_0, \hat{\mu}_0) = \frac{\partial}{\partial y} G(y_0, \hat{\lambda}_0, \hat{\mu}_0) = 0. \tag{14}$$

Eq. (14) yields the condition $\hat{\lambda}_0^2 = \frac{4}{27}\hat{\mu}_0^3$. Recalling that $\hat{\mu} = \mu + \varepsilon$ and $\hat{\lambda} = \lambda\sqrt{\mu}$, we get the locus of the bifurcation point:

$$\lambda^2 = \frac{4}{27\mu}(\mu + \varepsilon)^3, \tag{15}$$

which, unsurprisingly, follows from Eq. (8) obtained from the condition for the cubic polynomials in Eq. (12) to have exactly two roots.

Fig. 8 shows a two-parameter, (ε, λ), diagram of the locus of the bifurcation captured by Eq. (15) for a representative value of $\mu = 0.2$. For this particular value, the hysteresis point is located at $\varepsilon = -\mu = -0.2$. To the left of the locus of the bifurcation, there is only one equilibrium point, and it is stable. To the right of it, there are three equilibria, two of which are stable. The two additional equilibria are born at a saddle-node bifurcation, which is captured by the locus. The insets with the red markers showcase the transitions in the number and stability of the zeros of the polynomial $p_+(y)$ for a path in which ε varies while λ is held fixed.

Furthermore, since Eq. (15) is invariant under the change $\lambda \mapsto -\lambda$, then the transitions with $\lambda < 0$ are the same as those with positive λ. It follows that the locus of the saddle-node bifurcation applies identically to both $p_-(y)$ and $p_+(y)$.

4 A two-cell feedforward network of Stuart-Landau oscillators

In this section, we study the effects of inhomogeneities in the excitation parameter μ, the frequency ω, and the cubic nonlinearity parameter γ, in systems of two Stuart-Landau oscillators with a feedforward coupling. We first systematically study the case with an inhomogeneity in the natural frequency alone, as this paves the way for analyzing the system with inhomogeneities in all parameters. Then we add inhomogeneity in the excitation and nonlinearity parameters.

4.1 Inhomogeneity in the natural frequency

Fig. 9 shows a schematic diagram of a two-cell system with inhomogeneity in the frequency parameter.

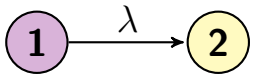

$$\begin{aligned} \dot{z_1} &= (\mu + i\omega) z_1 - |z_1|^2 z_1, \\ \dot{z_2} &= (\mu + i(\omega + \sigma)) z_2 - |z_2|^2 z_2 - \lambda z_1. \end{aligned} \tag{16}$$

Figure 9: A schematic diagram of a two-cell feed-forward network with Stuart-Landau cells with an inhomogeneity in the natural frequency represented by σ.

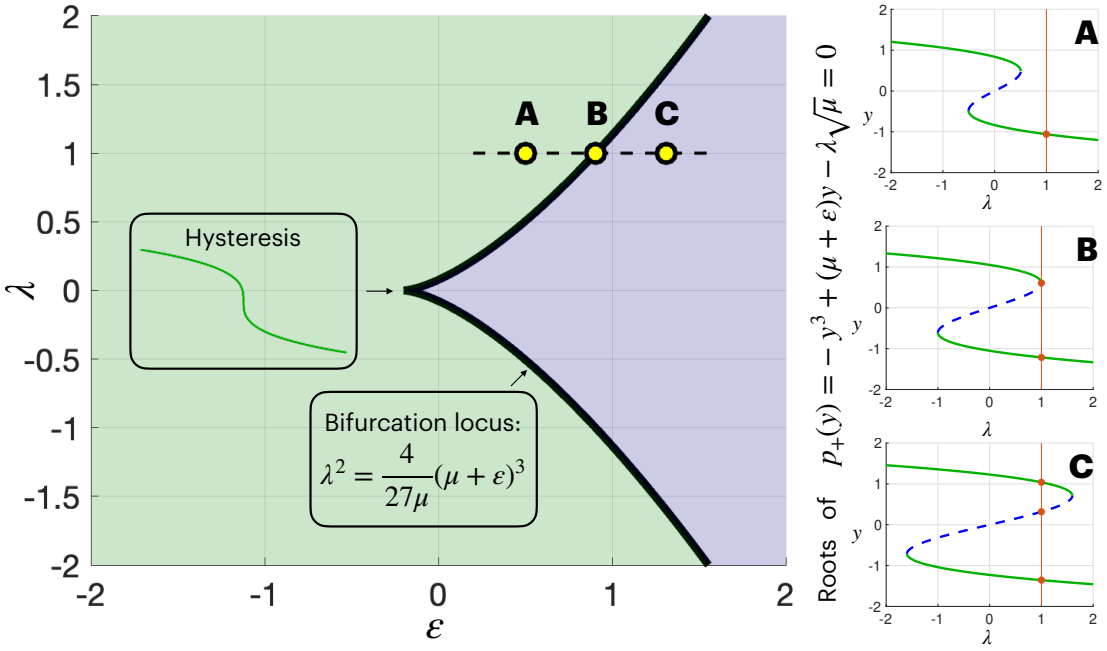

Figure 8: Two-parameter bifurcation diagram in the (ε, λ)-plane. Solid (green) curves in the insets indicate stable equilibrium points. Dashed (blue) curves depict unstable equilibrium points. The parameter μ was set to $\mu = 0.2$, as a representative example. For a fixed value of λ, for instance $\lambda = 1$, while varying ε from left to right, the number of equilibrium points (red filled-in circles in the insets), i.e., roots of $p_+(y)$, changes from one (to the left of the locus of a saddle-node bifurcation) to two (on the locus), and then to three (to the right of the locus).